Spec. Publs int. Ass. Sediment. (2001) **30**, 61–80

Eruption and reshaping of Pahvant Butte volcano in Pleistocene Lake Bonneville

J. D. L. WHITE

Geology Department, PO Box 56, University of Otago, Dunedin, New Zealand

ABSTRACT

Pahvant Butte, an isolated volcano that erupted in an arm of Lake Bonneville, is an outstanding example of the product of an emergent eruption, its interaction with water-level, erosion and deposition during eruption, and the volcano's response to post-eruptive water-level changes. Pahvant Butte consists of three distinct elements: a steep-sided tuff cone that consists of tephra deposited under damp and dry conditions, breached to the south-west, and having wave-cut cliffs on the north and west; a nearly flat-topped platform extending from the cone to the south and east; and a mound of generally well-bedded, shallow-dipping, subaqueously deposited tephra underlying and coring the platform. The morphology of Pahvant Butte is dominated by the cone and platform, with the mound truncated along the wave-cut cliffs and buried beneath the platform. The Pahvant Butte eruption began subaqueously, and the mounded strata formed largely before the lake surface was breached. Upon emergence, deposition became more localized around the vent, and the tuff cone began to develop. Both subaerial and subaqueous facies of steeply dipping cone strata are present; the latter provide a rare example of subaqueous fall-fed grainflow deposits. Erosion of the growing cone by waves and runoff rapidly shifted tephra to form the platform, which consists of lacustrine volcaniclastic beach spit, lagoonal, and local deltaic deposits. Such syn-eruptive platforms are characteristic of emergent eruptions, although their specific form and constitution depend on the interplay between eruptive activity and processes of erosion and redeposition. The Pahvant Butte eruption took place during the first Bonneville highstand; afterwards the lake level fell and rose again during the Keg Mountain oscillation, which involved a substantial fall in the level of the lake between the time it first reached the Bonneville shoreline and the final occupation of that shoreline before the Bonneville breakout flood. This rise was recorded at Pahvant Butte by stacked platform foresets.

INTRODUCTION

Pahvant Butte is one of a small number of volcanoes known to have erupted into the vast Pleistocene pluvial lakes such as Lake Bonneville (Fig. 1) that covered parts of the Basin and Range province of the western USA. These lakes were large bodies of water several tens of metres deep that have now disappeared or diminished, exposing both subaqueous and subaerial products of volcanoes in arid landscapes scarcely altered since the lakes' retreat.

The subaqueous to emergent volcanoes exposed by declining lake levels, such as Pahvant Butte, are ideal sites for investigation of subaqueous to emergent eruption processes and the interaction of waves, currents, and the eruption. Modern subaqueous to emergent volcanoes are difficult to study and their internal facies, particularly subaqueously developed ones, are not well known. Elsewhere remnants of shallow subaqueous volcanoes have been described (e.g. Cas & Landis, 1987; Cas *et al.*, 1989; Godcheaux *et al.*, 1992; Werner *et al.*, 1996; Smellie & Hole, 1997; Kano, 1998), but their original morphology is not well known.

Gilbert (1890) was probably the first to argue that Pahvant Butte volcano initially erupted beneath Lake Bonneville, an interpretation accepted by numerous later workers (Condie & Barsky, 1972; Wohletz & Sheridan, 1983; Oviatt & Nash, 1989; Farrand & Singer, 1992). Water depth at the site of eruption was ≈ 85 m (Oviatt & Nash, 1989; see further discussion below). The aims of this paper are:

1 to detail the development of the volcano's deposits and morphology, which reflect interaction of the lake

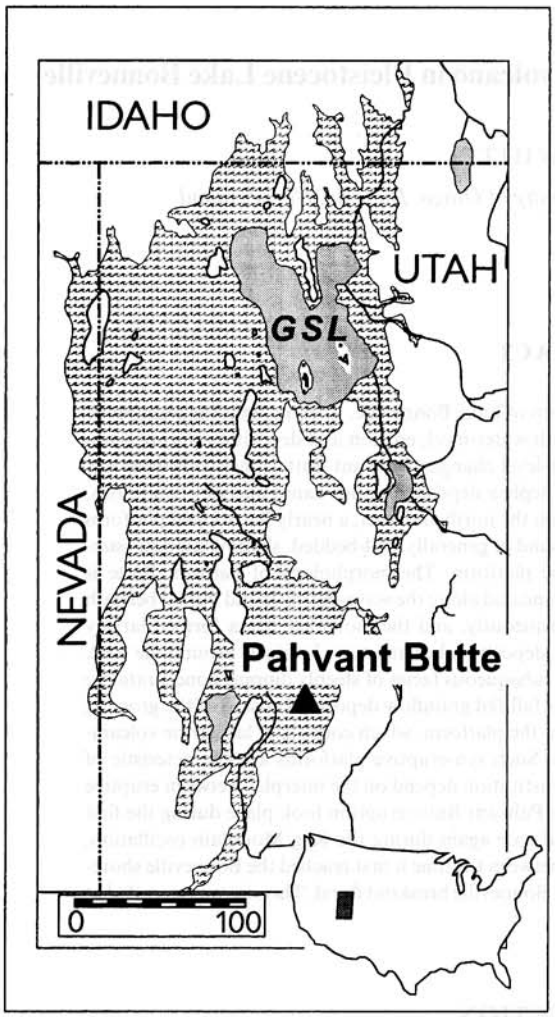

Fig. 1. Index map showing extent of Pleistocene Lake Bonneville at its highstand (patterned; after Currey, 1982). GSL is Great Salt Lake; similarly shaded bodies are other present-day lakes. Dashed lines indicate state boundaries of Idaho (ID), Nevada (NV), and Utah (UT). Pahvant Butte is located at 39.10°N, 112.55°W.

with eruptive and depositional processes both during and after eruption;
2 to evaluate the role of the lake's water in development of palagonitization;
3 to briefly address potential implications of the volcano's shoreline deposits for the history of Lake Bonneville. A related paper (White, 1996) provided a detailed discussion of the subaqueous phase of the eruption and its products.

Morphology and structural elements of Pahvant Butte

Pahvant Butte consists of three elements:
1 a complex, asymmetrical steep-sided tuff cone, breached to the south-west and having wave-cut cliffs on the north and west;
2 a nearly flat-topped platform extending from the cone to the south and east (Fig. 2), the margins of which consist of steeply outward-dipping beds of sideromelane tephra;
3 a broad mound of subhorizontally bedded tephra that is largely hidden beneath the platform (Fig. 3).
Several lines of evidence support the contention that Pahvant Butte erupted into the waters of Lake Bonneville, and was not simply reshaped by the lake waters subsequent to eruption (Gilbert, 1890; Oviatt & Nash, 1989). The most direct of these relate to the depositional features of the mound, which formed during eruption and below the inferred palaeolake surface (White, 1996).

The following sections address these elements in their general order of development, from subaqueous mound growth during eruption, through emergent eruption and formation of the cone, to platform and beach ridge development by lacustrine waves and currents. The ordering is a general one, however, because there was significant overlap among phases during the eruption.

THE MOUND

The earliest growth phase of Pahvant Butte is recorded by mound deposits largely hidden beneath the platform and cone. Defining characteristics of the mound deposits are shallow bedding dips (< 10°), and location low in the edifice, typically beneath steeply dipping cone strata. Mound strata consist of greenish sideromelane ash grains showing the wide range of vesiculation typical of phreatomagmatically disrupted vesiculating magma (Houghton & Wilson, 1989). The following summary of mound deposits is drawn from the more extended account of White (1996), in which the strata were assigned to four lithofacies associations and a detailed assessment of their origin was provided.

Lithofacies M1: well-bedded, broadly scoured coarse ash and lapilli

Lithofacies M1 (lithofacies association M1 of White,

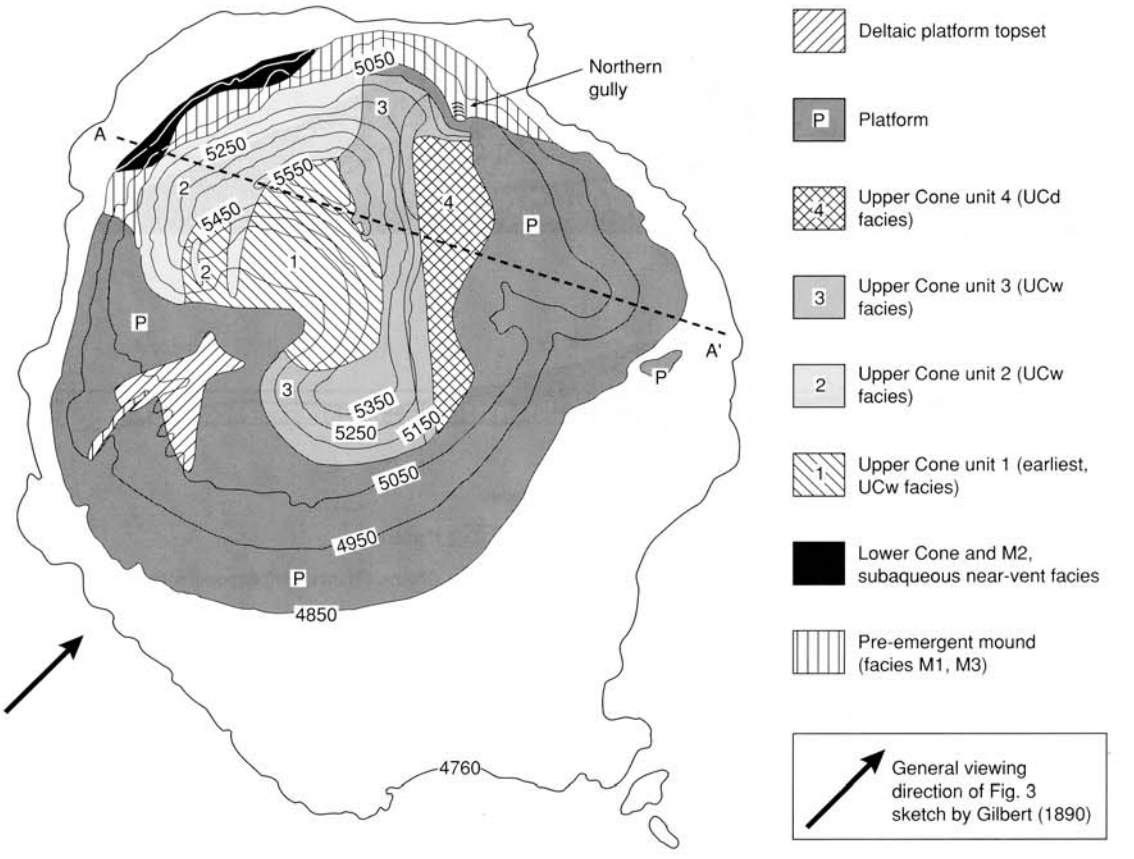

Fig. 2. Map of Pahvant Butte showing distribution of units described in text, and four upper cone assemblages separated by syn-eruptive slip surfaces (UC1, UC2, UC3, UC4). The deltaic platform topset grades into beach-spit deposits, both linked with platform foresets. Palagonite affects all units to varying degrees, and palagonitized zones are not mapped separately from fresh or cemented sideromelane tephra. A modern gully incised through deltaic topset and other platform deposits exposes a strip of mound deposits. Elevations are in feet, topography from USGS Pahvant Butte North and Pahvant Butte South 7.5′ topographic maps (1971; scale 1 : 24 000).

1996) was deposited directly on the lake floor ≈ 85 m beneath the lake surface, and consists largely of thin beds of coarse ash to fine lapilli. Broad scours, subtle bed lenticularity and very low-angle cross-stratification typify the M1 lithofacies (Fig. 4a), yet the thin beds are laterally continuous over tens of metres. Large clasts lie at or near the bases of beds without impact sags. Together these features suggest deposition from unchannelled, intermittently undercapacity and erosive (probably dilute), unsteady aqueous currents. These flows were capable of transporting a subpopulation of lapilli and small blocks and depositing them together with coarse to fine ash in a traction-dominated depositional regime.

Lithofacies M2: massive to weakly bedded lapilli ash with cauliflower clasts and armoured lapilli

Intercalated coarse ash beds and lapilli ash breccia beds make up lithofacies M2 (lithofacies association M2 of White, 1996), which is of limited extent and interfingers laterally with M1 and M3 beds. Lithofacies M2 differs from M1 in having definite sags beneath large particles (Fig. 4b), more diffuse bedding contacts, abundant armoured lapilli, and intercalated thick beds of coarse lapilli ash breccia bearing many clasts of deformed lake sediment (Fig. 4c). The bedding sags suggest ballistic emplacement of the larger blocks. Lapilli lenses above the block sags indicate

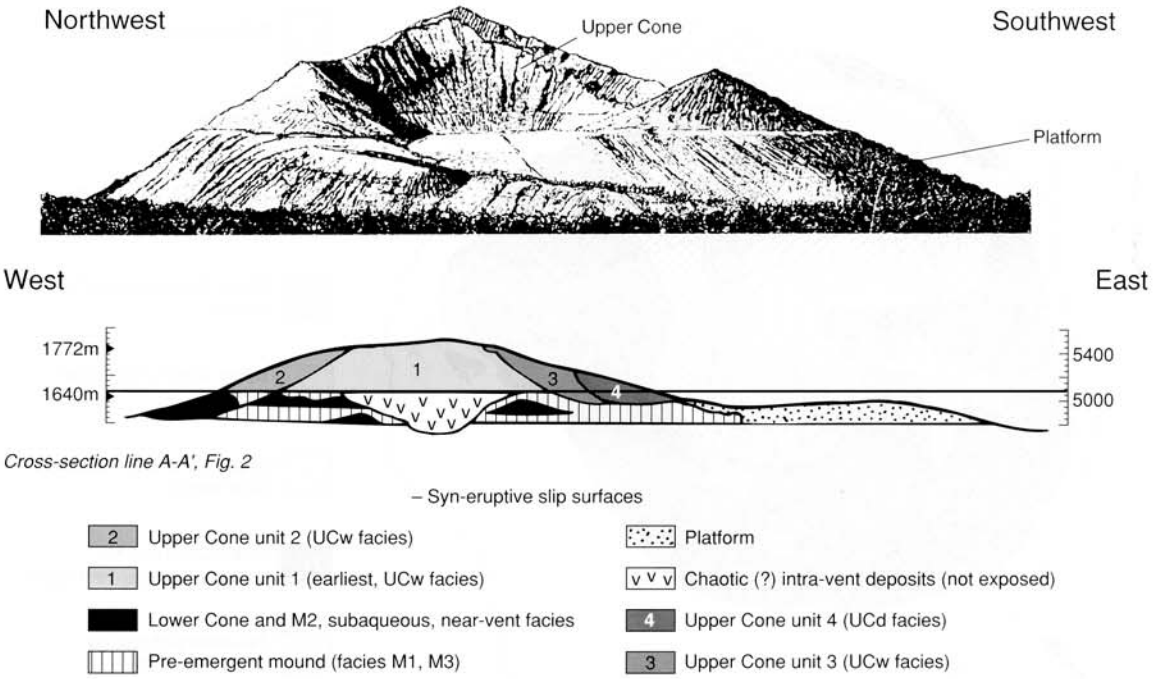

Fig. 3. Slightly modified version of Gilbert's (1890) field sketch, and interpretive cross-section of Pahvant Butte. View directions differ slightly, with cross-section plane chosen to emphasize platform deposits. Units are as in text and Fig. 2 except for addition of inferred chaotic intravent deposits, not exposed at Pahvant Butte. The M2 mound facies grade into lower cone deposits and are shown together. Upper cone units are separated by syn-eruptive slip surfaces, with younger cone units onlapping older ones across the slips. Lower cone and mound units are locally displaced along slips where exposed to the west and north.

lateral transport and emplacement of surrounding coarse ash, as do subtle bedding deflections around blocks and local erosion. Deposition was from sediment-gravity flows into which ballistic blocks were emplaced during flow. Diffuse internal contacts within thick beds are inferred to indicate sedimentation from high-sediment-concentration bases of sustained currents (Kneller & Branney, 1995). Lapilli lenses infilling above bomb sags are consistent with current deposition during bomb emplacement.

Lithofacies M3: broadly cross-stratified ash with local steep-foreset lenses and ripple-lamination

Moderately vesicular coarse sideromelane ash with intercalated lapilli ash and lapilli beds make up lithofacies M3, which generally overlies M1. Lithofacies M3 is overlain by ripple-marked beds that are, in turn, capped by primary subaerial tuff cone deposits (Fig. 3; see below). Very broad (≈ 1 m), low-amplitude (≈ 15 cm) dune-like bedforms (Fig. 4d) characterize M3. Cross-stratification, duneforms and rippleforms are well developed at higher levels, and extend to the uppermost exposures of the mound at palaeodepths of ≈ 20 m below syneruptive lake level. At greater palaeodepths, ≈ 50 m or more below lake level, facies M3 grades downward into M1. This facies developed by interaction between aqueous sediment-gravity flows and oscillatory flow beneath surface waves (White, 1996), and is present in strata that underlie rippled shoreline deposits and subaerial tuff cone beds; the facies formed before emergence of the volcano. Wave-generated oscillatory currents, superimposed on the outward flows, produced the form-discordant dune-like bedforms (White, 1996).

Lithofacies M4: thick-bedded, faintly stratified ash with rotated tuff blocks

Lithofacies M4 comprises thick beds of structureless to subtly stratified sideromelane ash and lapilli ash with reversely graded bases. It commonly contains

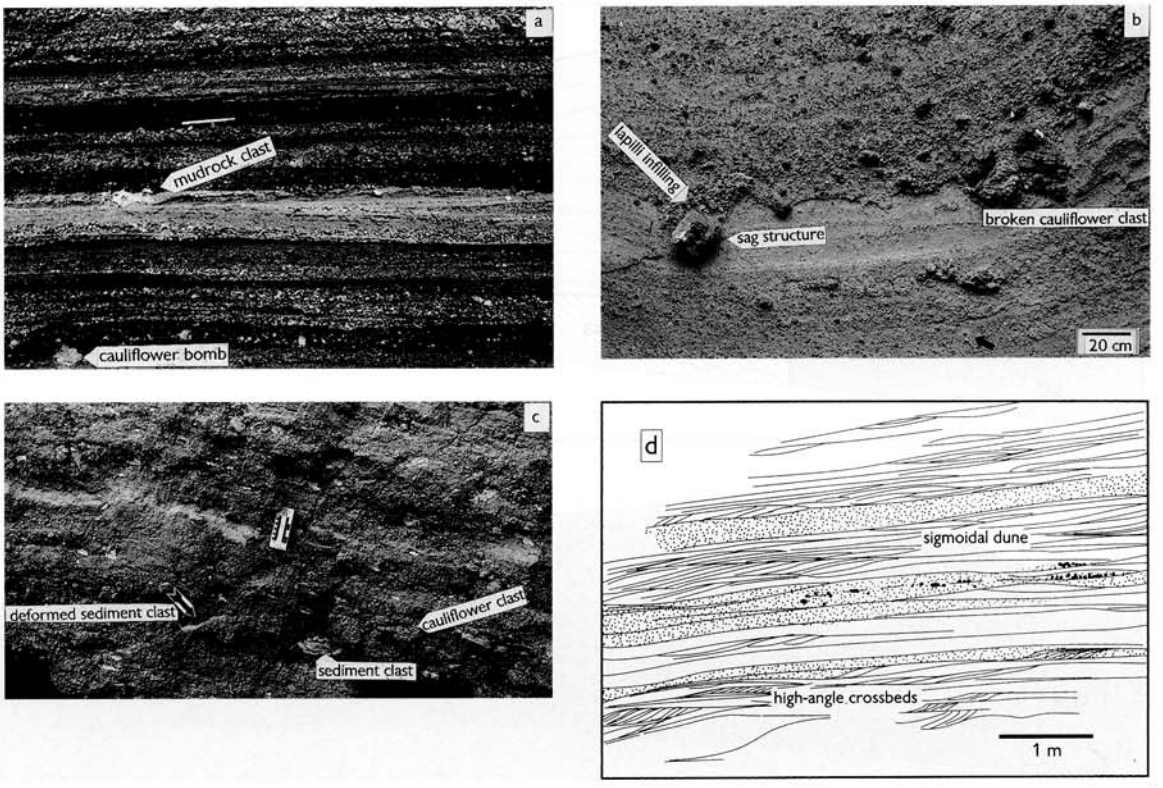

Fig. 4. Mound lithofacies. (a) Lithofacies M1, showing typical subhorizontal, subtly lenticular, bedding in the M1a lithofacies (pencil is 15 cm long). Dark beds are clean sideromelane ash, pale beds are carbonate-coated ash. (Note broad scour-and-fill near centre, irregular clast of lacustrine mud (now mudrock), and absence of sags beneath cauliflower 'bombs' near bottom of photograph.) (b) Lithofacies M2 showing horizon with cauliflower clasts, ash-rich layers containing armoured lapilli (arrow), white pieces of lacustrine mudrock (e.g. in and above broken cauliflower clast), and a sag structure infilled with lapilli (after White, 1996). (c) Lithofacies M2 lapilli breccia with scattered sediment clasts; some with lightly baked margins, others strongly deformed. (Note clast-supported texture, paucity of fine ash, and weak layering.) Cauliflower-textured juvenile clasts are present, characterized by rugged-surfaced glassy chill-rinds dissected by contraction-induced cracks. Left-hand bar on scale is 10 cm long (after White, 1996). (d) Lithofacies M3 showing broad, open dunes among subhorizontal beds with good lateral continuity and lenses of high-angle cross-strata (arrow). Bedding surfaces descend very gently to the left (to north-north-east, outward and downcurrent from cone).

rotated blocks of bedded ash, and is in contact with M1 and M3 lithofacies. Lithofacies M4 is the least characteristic of the mound lithofacies, and very similar deposits are also present in spit–deltaic foreset units of the platform, on the subaerial Pahvant Butte cone and on other emergent cones (Sohn & Chough, 1992). The rotated blocks of bedded tephra suggest partial disaggregation and flow of earlier ash deposits.

THE CONE

The cone consists largely of steeply dipping layers of poorly to well-bedded, originally glassy basaltic tuff, mostly altered to palagonite, and is interpreted as a fairly typical tuff cone. Subaerial parts of such cones have been widely described (Hamilton & Myers, 1963; Fisher, 1977; Leys, 1983; Wohletz & Sheridan, 1983; Verwoerd & Chevallier, 1987; Sohn & Chough, 1992, 1993), and are generally considered to form where magma erupts in the presence of surface water or abundant ground water (Heiken, 1971; Fisher & Schmincke, 1984).

Form of the cone

The strongly asymmetrical cone of Pahvant Butte is commonly described as having been breached in the

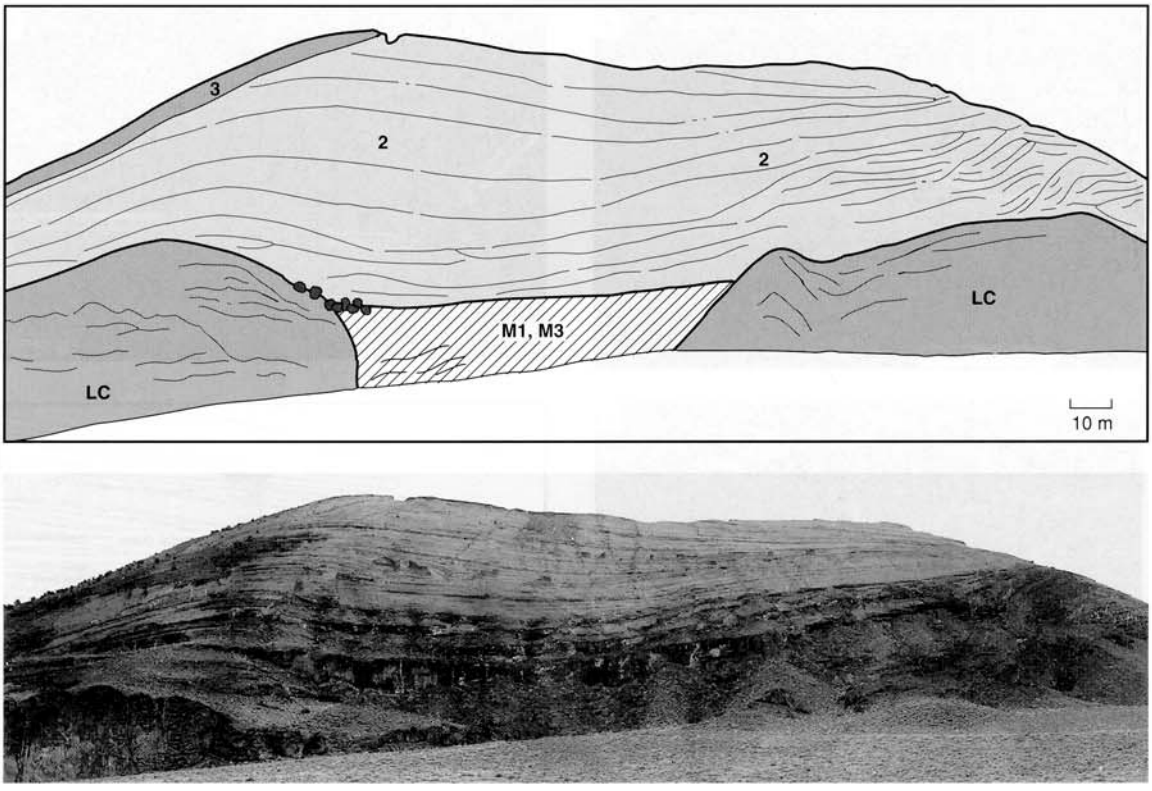

Fig. 5. Slightly oblique line drawing and photograph, taken from west-north-west of Pahvant Butte, showing anticlinal rim features of western rim segment. Prominent foreground cliffs were cut at Provo lake level. Left-dipping beds at upper left are UC3, in contact with UC2 across slip surface. Lower cone outcrops in cliff have more massive aspect.

south, where the platform is broadest and no cone wall is present (Gilbert, 1890; Wohletz & Sheridan, 1983; Oviatt & Nash, 1989). The western part of the cone rises and broadens northward toward the summit, from which it descends to a low saddle in the northeast before rising again to a subconical hill that terminates the cone to the east-south-east (Fig. 3). Two low anticlinal features underlie the north and south ends of the segment and are spectacularly draped by overlying cone beds (Fig. 5).

The shape of the cone is not easily explained in terms of westerly winds documented as prevalent during eruption (Oviatt & Nash, 1989), or by lacustrine erosion of the edifice (evaluated in more detail below). The low anticlinal features may represent part of an earlier rim, the western edges of which have been eroded and eastern ones buried beneath the larger cone. To the south, the absence of a cone wall probably results from a combination of weak initial development (unfavourable winds or significantly inclined vent), slip failure, and erosion and burial as the platform developed.

Depositional features

Lower cone

Lower parts of the cone are locally exposed in cliffs below the 5050 ft (1540 m) contour (Fig. 3), and have relatively steep bedding dips (≈ 20°). Beds vary in thickness from ≈ 2 to 20 cm, characteristically have diffuse contacts, and are lensoid and discontinuous (Fig. 6).

The reverse-graded beds and lenses in steeply dipping strata composing the lower cone suggest emplacement by grainflow processes (Nemec, 1990; Sohn & Chough, 1993), but the beds are not nearly as lenticular, nor as steep, as those constructed subaqueously by avalanche processes at angles of repose (Buck,

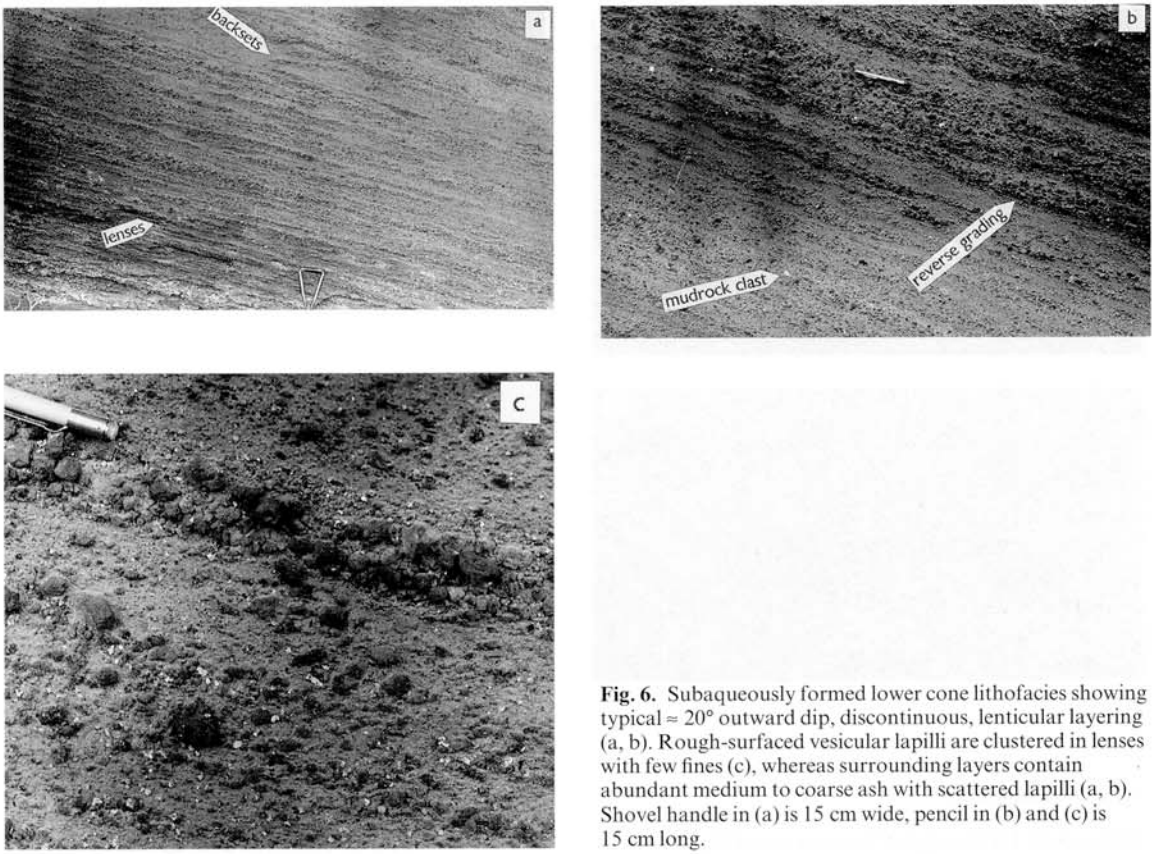

Fig. 6. Subaqueously formed lower cone lithofacies showing typical ≈ 20° outward dip, discontinuous, lenticular layering (a, b). Rough-surfaced vesicular lapilli are clustered in lenses with few fines (c), whereas surrounding layers contain abundant medium to coarse ash with scattered lapilli (a, b). Shovel handle in (a) is 15 cm wide, pencil in (b) and (c) is 15 cm long.

1985; White, 1992). This facies is inferred to have been deposited by grainflows that evolved from fall sedimentation (Sohn & Chough, 1993), but on the lower cone this process occurred subaqueously. The subaqueous setting, in conjunction with vesicular pyroclasts, has two important effects:

1 particle fall velocity is reduced relative to subaerial settings;

2 stability of depositional slopes is reduced, as a result of the loose packing and low density contrast between particles and interstitial fluid.

It is inferred that these effects counteract each other in forming subaqueous suspension-fed grainflows; slower settling greatly reduces initial saltation effects compared with subaerial settings, but the slope instability results in an intermittently mobile surface layer into which incoming particles are entrained.

Upper cone

Beds of the upper cone dip steeply (typically 20–30°, but up to 35° locally), and are strongly overprinted by palagonitization (see below). Two lithofacies are distinguished, each comprising a genetically related group of beds. They form parts of four slip-bounded assemblages that developed as a result of instability during construction of the subaerial cone.

Lithofacies UCw

Lithofacies UCw is characterized by block and bomb sags, and by accretionary and armoured lapilli (Fig. 7). Beds typically have impact sags, often contain armoured lapilli, and show generally poor bedding continuity and definition. Duplex structures and structureless tuff with rotated bedded tuff blocks locally fill concavities formed by slope failure. Pronounced rill erosion locally produced small deeply incised channels, typically 10 cm wide and as much as 50 cm deep, with inter-rill spacings of less than 1 m. The rills are most commonly infilled with lapilli tuff.

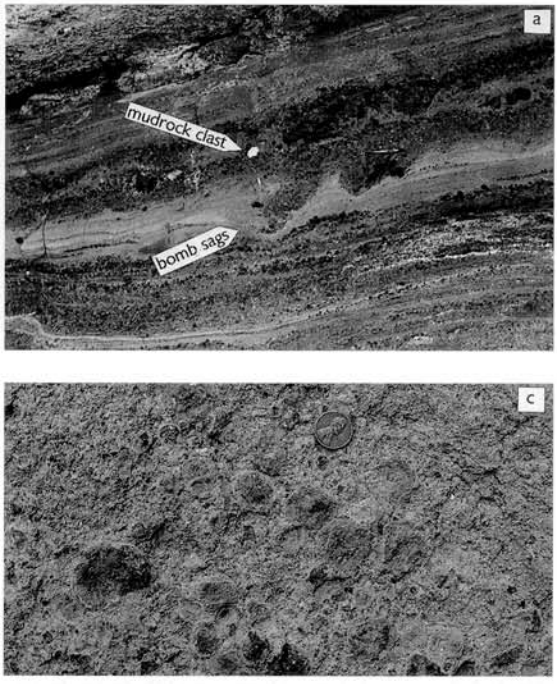

Fig. 7. Subaerial cone lithofacies UCw, with sag and accretion features. (a) Mixed fine- and coarse-grained horizons with white lacustrine mudrock clasts, and pronounced bedding sags beneath cauliflower texture bombs. (b) Backset-stacked lapilli tuff, formed syneruptively by duplex slip faulting. (c) Cored accretionary lapilli from same site as (b). Coin is 2 cm in diameter.

UCw interpretation

Features of UCw suggest transport and deposition of tephra in the presence of water. The damp ash was cohesive, and coated coarser clasts during their transport from the vent to the depositional site to form armoured lapilli. Layers of damp ash were sufficiently cohesive to produce well-developed sags beneath ballistically emplaced blocks, and to maintain local bedding coherence during failure (Fisher & Schmincke, 1984); the beds were partially disaggregated during flow to form rotated blocks in debris-flow deposits (Lorenz, 1974). Local duplex bedding reflects slip failure of damp ash, which stacked against the downslope margins of slip surfaces (Sohn & Chough, 1992). The localized deep rilling resulted from the downslope flow of water, either released from very wet tephra or thrown from the vent as 'free' water during eruption (Verwoerd & Chevallier, 1987). It is inferred that the association was produced largely by deposition from cock's tail plumes or jets, which deposit material by a combination of ballistic emplacement and subsynchronous rapid fallout (Thorarinsson, 1967; Sohn, 1996), with a lesser contribution from low-energy pyroclastic density currents.

Lithofacies UCd

Lithofacies UCd is characterized by thinly bedded, interstratified layers of framework-supported fines-poor coarse ash and lapilli together with thin ash layers (Fig. 8). Reverse grading is locally prominent in the openwork lapilli layers. Local scours are filled by broadly concave-upward lenses of fines-poor ash. In places, decimetre-thick beds of coarse ash contain 2–5-cm basalt lithic clasts, either concentrated in small lenses at bed tops or scattered randomly within beds. These are interlayered with thin, continuous ash layers a few millimetres thick. Swarms of small ventward-dipping normal faults occasionally cut the ≈ 25–$30°$ dipping beds. Beds of UCd lack accretionary lapilli, bomb sags, and other evidence of dampness upon deposition.

UCd interpretation

Grainflow and fallout processes are inferred to have produced features observed in UCd. The lack of particle cohesion suggests that little or no water was present upon deposition or during transport. Lithic clasts without accompanying sags, within or at the tops of

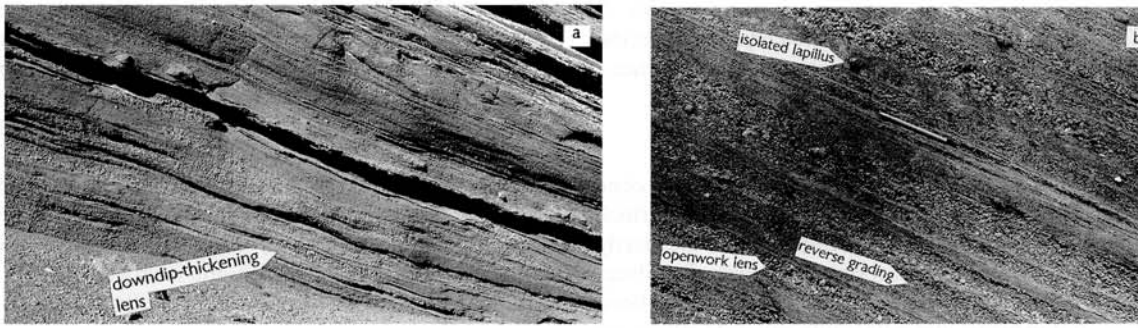

Fig. 8. Subaerial cone lithofacies Ucd, formed in late stages of the eruption, is characterized by (a) steep dips and sharply defined bedding, and (b) conspicuous lenses of openwork lapilli with laminae of fine tuff. Thin beds of fine to coarse tuff in places contain isolated lapilli; separate layers and lenses of fines-poor lapilli show both normal and reverse grading; there are clast-cluster fabrics and local down-dip coarsening.

sandy tephra beds, suggest emplacement by grainflow. Thinly laminated ash is suggestive of settling from suspension. Isolated larger clasts in thinly laminated strata rolled or bounced into place.

During deposition of UCd the vent was probably at or near the surface of the lake, and protected from direct water influx by a tephra dam. The resulting eruption ejected hydroclasts with little early condensing steam or water, allowing relatively effective sorting in the eruptive column and/or fallout plume. By analogy with observed processes at Surtsey, the most likely eruptive style associated with these 'drier' deposits might be one of continuous uprush. This fails, however, to explain the closely spaced ash laminations and generally thin bedding. It is more likely that reduced access of water to the vent in this case did not coincide with increased eruptive rates, and the result was a simple transition toward 'dry' phreatomagmatic activity. In addition to fall-fed grainflow, deposition of some thinner and less lenticular beds is inferred to have occurred from bases or tails of surges moving down the steep volcano flanks (Crowe & Fisher, 1973; Sohn & Chough, 1989). The finest-grained laminae are interpreted as fall deposits.

The restriction of recognized UCd strata to the last-formed cone deposits suggests that 'dry' phreatomagmatism was significant during only the closing stages of the eruption. There is no a priori reason to expect that UCd strata would be preferentially removed, and, despite the pernicious effects of palagonitization (see below), bomb sags, armoured lapilli and other dampness-related features are ubiquitous in earlier beds.

Syn-eruptive cone deformation

Three extensive slip surfaces, each overlain and onlapped by younger tephra beds, demarcate facies assemblages and help define the shape of the Pahvant Butte cone (Figs 2 & 3). The oldest recognized slip surface truncates the UC1 assemblage of upper cone tuffs and is inferred to displace some lower cone deposits. Another slip surface dips inward and encircles much of the inner slope of the cone. The youngest dips outward and truncates outward-dipping beds along the north-eastern segment of the cone. All are mildly upward-concave, with very steep upper surfaces that shallow only slightly before passing out of view beneath the platform. In addition to these large slip surfaces, early failure has locally produced chaotic beds up to 5 m thick with irregular, scoop-shaped, discordant lower contacts and rotated blocks of bedded tephra in a structureless tephra matrix. Locally, small-scale, outward-dipping subvertical reverse faults offset beds by < 10 cm; much of the offset is taken up along sharp flexures, and the faults die out upward within UC4 beds.

Repeated slip-failure is a characteristic accompaniment to growth of emergent Surtseyan volcanoes (Lorenz, 1974; Kokelaar, 1983); it is facilitated by depositional oversteepening as wet, jetted material is deposited by fall, and by the effects of shaking and surface impact of the jetted material (Sohn, 1996). Pervasive small-scale faulting is absent at Pahvant Butte (see Sohn & Chough, 1992). Localization of deformation along a few large slips involving UCw deposits suggests that the damp deposits were

coherent upon or soon after deposition (Sohn & Chough, 1992), and rafts of bedded tephra within the chaotic beds similarly suggest early stratal coherence.

Palagonite

Strong palagonitization is characteristic of the cone deposits except for an impersistent, decimetres-thick upper crust held together by a finely crystalline, partly geopetal, pore-lining carbonate cement. In places palagonite formed preferentially within specific horizons, but in many sites palagonite zones steeply cross-cut bedding boundaries. Over the whole of the cone, bed-specific palagonitization is strongly subordinate to more general alteration that is independent of both bedding and depositional facies. None of the slip surfaces consistently separate palagonitized from non-palagonitized zones, nor are rotated blocks of bedded tephra in chaotic beds preferentially palagonitized.

In parts of the lower cone deposits, and locally in the inner part of the platform deposits where their contact with lower and upper cone beds is exposed (see below), palagonite zones steeply cross-cut bedding and grade from almost fresh glass, to palagonite rims, to palagonitized particles, to fully palagonitized tephra in which a pervasive pseudomatrix of zeolites and clays has completely infilled the original pore space. Differences in appearance between palagonitized and non-palagonitized parts of individual beds are pronounced, with the latter appearing much more matrix rich in outcrop, hand specimen and thin section (see Hay & Iijima, 1968). The effect is so strong that originally openwork, virtually ash-free beds of lapilli appear, where palagonitized, to consist of coated lapilli supported by an ashy matrix. Where clasts are moderately or strongly vesicular, palagonite often forms broad rims grossly similar in appearance to accretionary coatings.

Pahvant Butte has been cited by some workers as an example of palagonitization controlled by depositional processes and restricted to beds formed by subaerial deposition of wet ash (Wohletz & Sheridan, 1983; Farrand & Singer, 1991, 1992; Wohletz & Heiken, 1992). The cross-cutting palagonite zones that affect the cone, however, indicate that the palagonitization is not systematically related to depositional facies. The distribution and characteristics of Pahvant Butte palagonite and the surficial unpalagonitized layer closely match those of Hawaiian examples (Hay & Iijima, 1968) that are inferred to have formed by ground-water alteration of sideromelane tuffs without regard to specific depositional facies. Moreover, steeply orientated zones of palagonite that locally cut across lower cone deposits show that the process also took place below the lake surface, in more interior regions, almost certainly as a result of hydrothermal activity (Jakobsson & Moore, 1986). Absence of palagonitization in most of the platform deposits (below) probably results, as in Hawaii, from a position below the Pleistocene water table (lake level) and beyond zones of hydrothermal activity, and from the relatively arid post-pluvial climate of the Pahvant Butte area.

PLATFORM

The Pahvant Butte platform is asymmetrically arranged about the tuff cone, and its surface lies at ≈ 5050 ft (1540 m) elevation (Figs 2 & 3). No platform is present at the north-west side of the cone, where high, wave-cut cliffs extend to the base of the cone. To the south-east the platform extends over the presumed site of the major vent. An elongate tongue of the platform extends to the south-east along its north-eastern edge, and is capped by a pronounced beach ridge. The elongation of the tongue, the capping beach ridge, and the down-tongue dip of large-scale (> 20 m) foreset beds suggest that the tongue formed as a drift-aligned beach spit (Gilbert, 1890; Carter *et al.*, 1991).

Both the large-scale distribution of ash from the eruption (Oviatt & Nash, 1989) and the high north-west–south-east semicircular cone rim suggest winds from the south to south-west during the eruption and growth of the cone. Wave-cut cliffs on the north-west of the cone, and the drift-aligned spit extending to the south-west, however, suggest that waves from the west to north-west were predominant during platform development. This might result from seasonal wind shifts, with strongest winds, and thus maximum wave energy for reworking and platform growth, occurring during winter as storms moved in from the north-west. Late-stage lacustrine erosion, which probably occurred at the 4750 ft (1450 m) 'Provo' shoreline (Gilbert, 1890; Oviatt & Nash, 1989), significantly steepened the margins of the platform and in the process truncated the beds forming its lower part.

Progradational beach deposits, local delta

The platform is partly encircled by a capping beach ridge, and strong drift alignment of the north-eastern tongue (Fig. 3) suggests that this part of the platform

is a spit complex, formed primarily by downdrift beach progradation (Nielsen *et al.*, 1988). South-west within the breached cone, however, the marginal topset beds show outward-dipping, metre-scale, planar–tabular cross-beds that record progradation of microdeltaic transverse bars at the mouths of feeding streams, and indicate that progradation at that site was not controlled by the direction of beach drift. This south-western part of the platform was abundantly supplied with sediment from the erosion of the cone, and it prograded southward as a delta with comparatively minor downdrift redistribution of the sediment by beach processes.

The platform foresets consist of both progradational beach and deltaic deposits, but the subaqueous foresets are identical in both spit and deltaic deposits (see Nielsen *et al.*, 1988), a reflection of the very limited transport and reworking in both beach and delta systems. In recognition of this kinship, the platform is here considered to include the large-scale foreset beds of both deltaic and prograding beach origin. It is topped by deltaic and/or beach (spit) topset deposits (see Nielsen *et al.*, 1988; Chough & Hwang, 1997).

Main platform topset

Delta

The deltaic topset that forms much of the south-western, and part of the north-eastern, platform is exposed only in scattered outcrops along the platform periphery. Along the western to southern edge it consists of ≈ 2-m-thick, tangentially based planar–tabular cross-beds overlying a few-metres-thick sequence of flat-bedded tuff (Fig. 9), which locally contains ripple marks, rootlet casts, and subhorizontal burrows. The foreset bedding is steep (25–30°), and locally contains lenses of backset beds that typically consist of openwork lapilli. The cross-beds in marginal topset strata generally dip toward the platform margin, but in one, more inward location near the expected location of the now-absent southern wall of the volcanic cone (Fig. 2), foreset strata dip down the axis of a large ravine that evidently follows an earlier subaqueous sediment pathway. Sediment for the delta was presumably provided by small-scale rills and shallow gullies cut into the originally unconsolidated ash

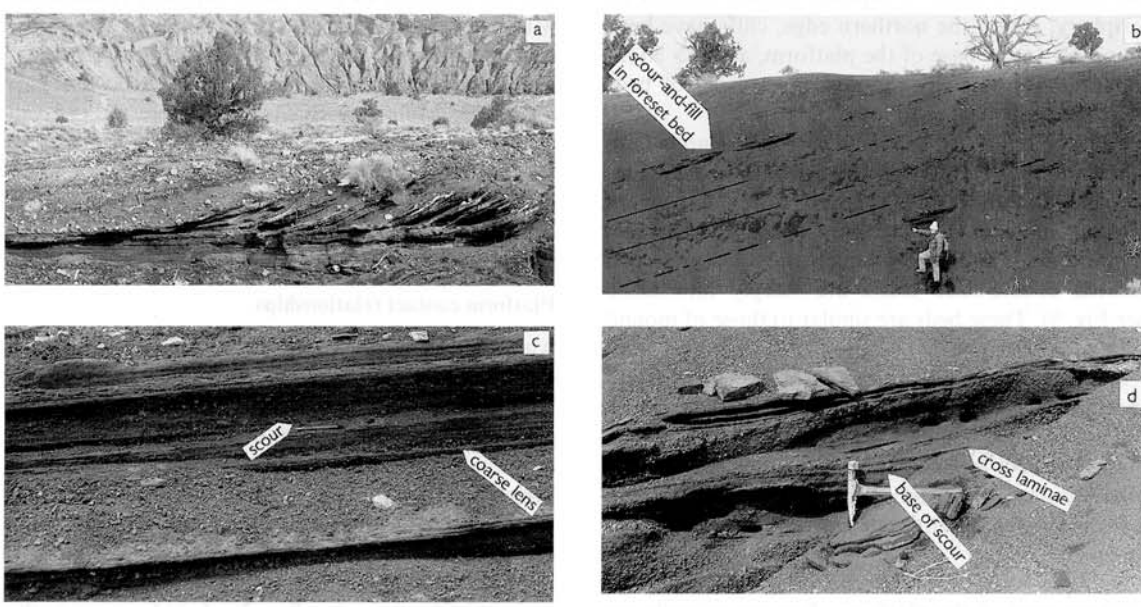

Fig. 9. Platform features: (a) west-dipping deltaic foreset beds (≈ 1 m tall) on south-western platform, hammer for scale; (b) larger-scale deltaic foreset beds dipping outward along south-western gully, fine-grained beds more resistant; R. V. Fisher for scale; (c) typical foreset beds showing subtle lenticularity as a result of shallow scouring, lenses and layers of openwork lapilli, and good general continuity of intercalated medium- to fine-grained ash beds (pencil 15 cm long); (d) close-up of scour infilled by cross-laminae in foreset bed (hammer is 30 cm long).

(Segerstrom, 1950; Ollier & Brown, 1971), but none are preserved; larger gullies may have formed, but are not distinguishable from modern topography on the lithified remnant of the cone.

Beach and spit

The deltaic topset beds grade eastward into elongate gravel mounds that top two protuberances along the eastern margin of the platform. The ridges are interpreted as beach spits, one that advanced northward around the eastern margin, and another that extended eastward. They are separated by a deep gully that funnelled sediments from the narrow eastern platform down the flank of the platform (Fig. 2). Limited exposure along the upper edges of the spits shows steeply dipping (≈ 25°) beds, 2–10 cm thick, that dip outward and strike parallel to the platform margin. Within the re-entrant between the spits, thin beds of fine-grained, intensely rippled ash exposed a few metres below the platform margin represent deposition in a protected re-entrant between the prograding spits.

Platform foreset

The platform foreset is exposed mostly around its periphery. Along the northern edge, cliffs have been cut nearly to the base of the platform, and a > 30-m-tall foreset is partially exposed. Two types of beds make up the foreset, as follows.

1 Thick beds (0.5–1.5 m) of coarse ash and lapilli have subtle internal layers defined by discontinuous, gradational to slightly erosive, planar to weakly scoured contacts, and elongate 'stringers' of lapilli. The bases of some thick beds show liquefaction features, and isolated cobble-sized clasts are steeply imbricated (see Fig. 9). These beds are similar to those of mound lithofacies M4.

2 Medium beds (1–50 cm) of interlayered coarse- and finer-grained ash have bedding surfaces that are generally flat to slightly undulose, commonly with eroded bases. The beds typically have very low-angle internal cross-stratification defining broad, low bedforms a few centimetres in amplitude and with wavelengths of a metre or so.

Multiple foreset units can be recognized along the southern part of the platform. Two upper units are exposed along the southern margins, and each is 10–15 m high and tangential based, with dips as steep as 25° near its crest (see Fig. 9). This large-scale foreset bedding unit generally dips toward the platform margin, but is locally diverted, in the same sense as the topset-bed cross-strata, along earlier subaqueous sediment pathways. The upper parts of the foresets are steep (25–30°), and discontinuous layers of openwork lapilli locally form backset beds. The foreset units are separated by locally ripple-laminated topset beds. The upper foreset unit is stacked atop the lower foreset unit (see *Discussion*).

Foreset sedimentary features and sedimentation

Bedforms are similar throughout the platform foresets. Broad, low-angle dunes and swales, with subtle internal stratification defined by thin, lenticular lapilli horizons, are characteristic, and indicate ubiquitous erosion and downslope traction transport on the foresets. High-concentration turbidity currents, cohesionless debris flows, and occasional debris falls (Nemec, 1990; White, 1992; Kim *et al.*, 1995) are inferred to have been the primary means of sediment transport down the platform foresets. Bedform suites resulting from these processes may represent both lower-beachface sediments (Massari & Parea, 1988) and delta-front deposits (Nemec, 1990; Kim *et al.*, 1995), depending on the nature of the sediment delivery to the upper foresets. The Pahvant Butte platform foresets are inferred to have been supplied episodically with sediment, by storm-wave entrainment and downslope density flow (Nielsen *et al.*, 1988), hyperpycnal streamflow (Prior & Bornhold, 1989; Orton & Reading, 1993; Mulder & Syvitski, 1995) resulting from rainfall on the cone, or by slumping of the upper foreset induced by depositional oversteepening or wave loading (Massari, 1984; Postma, 1984; Prior & Bornhold, 1990).

Platform contact relationships

Although the lower contact of platform strata with underlying and adjacent mound and cone strata is largely obscured, a section exposed in the northern gully (Fig. 2) offers important insight into the nature of the relationship. In the deep gully, a complex relationship between cone, mound and platform strata is revealed (Fig. 10). The lower levels of the gully expose undulose-bedded M3 mound strata. Upward, bedding becomes more complex, with high-angle cross-stratification locally developed among the undulose beds. Slightly more upsection, and somewhat closer to the vent, strong palagonitization sets in at approximately the same level that very complex bedsets of ripple cross-laminated strata, sharp erosional troughs, and an onlapping unit of more steeply

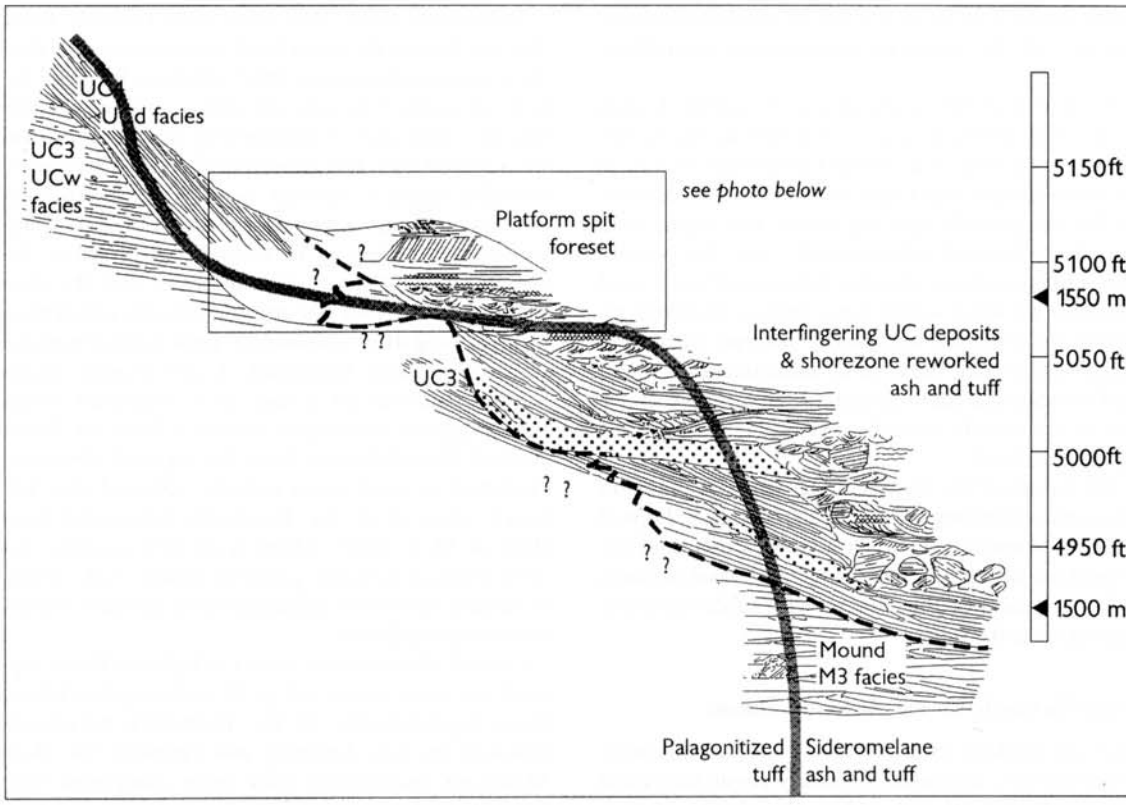

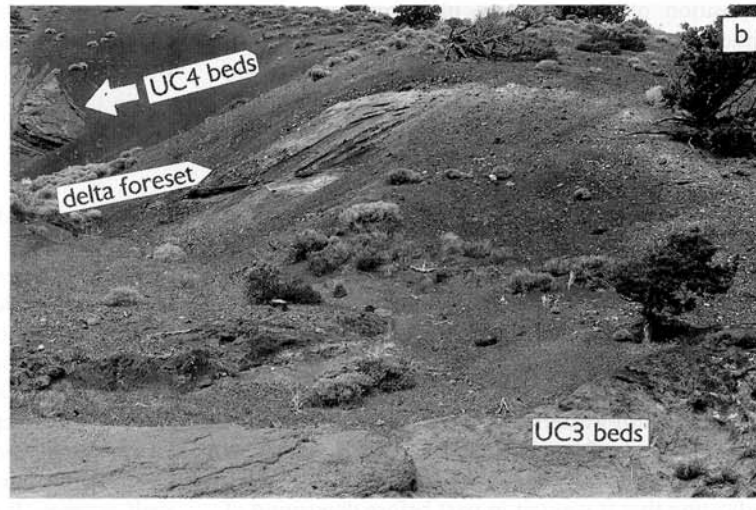

Fig. 10. Contact relationships from northern gully (see Fig. 2). Schematic, vertically exaggerated diagram (a) summarizes relationship of mound, upper cone, and platform strata. The thick black line separates palagonitized tuff to the left from non-palagonitized tuff and tephra to the right. Photograph (b) looks toward the cone and shows topset–foreset transition near 5100 (1555 m) ft elevation; tuff of the UC4 assemblage in the background dips toward the viewer, and palagonitized tuff of the UC3 assemblage in the foreground is intercalated with rippled syn-eruptive shore-zone platform deposits.

dipping, thin-bedded strata appear. The latter are in turn sharply incised and overlain by a unit of a few metres thickness that consists largely of broken-up bedded tuff blocks.

The erosional contact between inferred cone strata and overlying ripple-laminated and trough cross-bedded units strongly suggests that this complex zone represents a syn-eruptive shoreline. Syn-eruptive development is demonstrated by the offlapping relationship of the overlying, also truncated, steeply dipping strata,

which are taken to be part of the UCd lithofacies cone deposits of the youngest depositional assemblage (UC4).

At 5120 ft (1560 m) elevation, the topset–foreset break of a deltaic foreset is exposed in the north-western gully (Fig. 9) at a level higher than the top of the north-eastern beach-spit berm (5085 ft (1550 m)). Unlike the gravelly spit-top berm, the topset beds must have formed subaqueously, and the topset–foreset break is thus a sensitive indicator of water level preserved in what would have been a sheltered re-entrant along the nor-thern shore. Because it is several metres higher than the zone of intercalated UC4 and platform deposits that represent a syn-eruptive shoreline, it apparently records a (brief?) post-eruptive higher lake stand.

The nature of the basal contact between platform strata and underlying mound strata is obscure. Dips of platform foreset strata shallow downwards, and the foresets are inferred to have tangential basal contacts and thus a conformable contact with subhorizontally dipping mound strata.

Bonneville lake levels and platform evolution

The local stacking relationship of multiple tangential-based foresets, separated by locally ripple-laminated topset beds (Fig. 10, and see Fig. 11, below), indicates deposition of the observed platform-margin units under rising lake levels (see Chough & Hwang, 1997), recording stages of normal constructional regression (shoreline outbuilding) and rapid, non-accretionary transgression (drowning; Helland-Hansen & Martinsen, 1996). The stacked foreset units record small-scale lake-level changes, and may have formed as Lake Bonneville rose after a brief fall termed the Keg Mountain oscillation (Fig. 12), which is inferred to have taken place not long before initiation of the Bonneville Flood and resultant rapid lowering of the lake to the Provo level (Bills & May, 1987; Sack, 1989; Oviatt *et al.*, 1992, 1994).

Local incision and eastward longshore drift occurred along the south-western margin of Pahvant Butte during the fall and subsequent lake-level rise. Foreset beds of the upper foreset unit advance along this gully, indicating that it was cut in part before deposition of the unit. Sediment carried down and deposited at the mouth of this gully forms a poorly exposed but morphologically distinct wedge, clearly illustrated as an eastward-sloping ridge in front of the main platform in Gilbert's (1890) engraving (top frame of Fig. 3).

Indications from sites other than Pahvant Butte that the Bonneville water level continued to rise after the eruption (Oviatt *et al.*, 1992, 1994) are based on the best estimates of the ages of eruption and catastrophic lake lowering, and on stratigraphy of ash deposits in the Sevier Desert. It is important that the syn-eruptive shoreline features exposed along the northern gully of Pahvant Butte require that the top of the platform was approximately at or several metres below the syn-eruptive lake level. This indicates that the platform originated as a syn-eruptive feature, rather than forming long after eruption by prolonged reworking at the Bonneville highstand. A syn-eruptive origin for the platform (at a lake level somewhat below the Bonneville maximum) reduces a Pahvant Butte-centred 17-m deflection from the regional elevations predicted to result from isostatic rebound that followed removal of the Bonneville lake-water load (Bills & May, 1987). There is no field evidence for 'post-eruptive volcanic collapse' (Bills *et al.*, 1994), so several metres of deflection from predicted levels remains unexplained.

Overall, the shoreline record at Pahvant Butte supports the curve shown in Fig. 11, with eruption taking place approximately at the Bonneville maximum, followed by lake lowering and renewed rise (Keg Mountain oscillation?) that were associated with stacked platform foresets, and a last brief rise to a maximum recorded by the small deltaic topset–foreset contact before the final lake-level drop caused by the Bonneville flood.

DISCUSSION

Even large and deep lakes are commonly short-lived bodies of water (Talbot & Allen, 1996), with less severe wave regimes than most oceanic settings. The result is that volcanoes erupted subaqueously within lakes are commonly preserved and exposed to view with only minor modification (e.g. Gilbert, 1890; Christensen & Gilbert, 1964; Tazieff, 1972). Pahvant Butte is an exceptionally well-preserved example of an emergent volcano (Kokelaar, 1986), erupted at a water depth equivalent to those of typical marine shelf settings. It records a sequence of eruptive and sedimentary events (Fig. 11) typical of that which shapes marine volcanoes of island arcs (Hoffmeister *et al.*, 1929), shallow spreading ridges (Richards, 1959; Thorarinsson, 1967), and coastal continental intraplate settings (Coombs *et al.*, 1986).

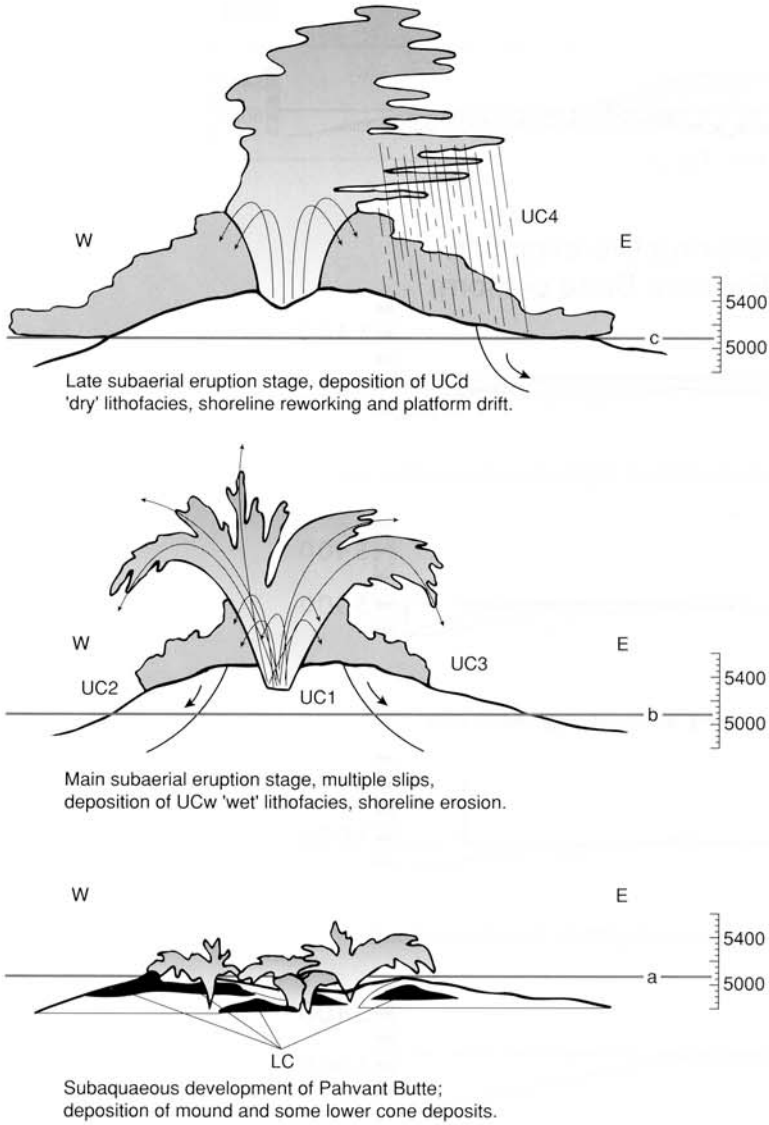

Fig. 11. Summary illustration of Pahvant Butte's history in Lake Bonneville: (a) Eruption begins under ≈ 85 m of water, producing a low mound of tephra before eruptive emergence (White, 1996), and development of M2 and lower cone deposits (depending on nature of eruptive column) at vent margins. Multiple vent sites are inferred during this stage. (b) The volcano emerges above lake level, but full access of water to the eruption site continues, feeding UCw 'wet' phreatomagmatic deposits fed largely by tephra jets (cock's tail plumes). Parts of the cone fail along broad slip surfaces, some soling deeply enough to displace mound and lower cone deposits. Slip surfaces are mantled and onlapped by continuing tephra jet deposition. (c) In the late stages of eruption, lessened access of water to the vent is indicated by development of UCd 'dry' phreatomagmatic deposits, fed by grainfall and deposition from the base of expanded density currents carrying little or no condensed water. (d) This and later frames show only the eastern spit area (box at top; Figs 2 & 3). Early spit growth occurs at the syn-eruption lake level, probably very rapidly. (e) Following the close of eruption and early platform building, lake level drops during the Keg Mountain oscillation. A topset unit develops at a lower elevation than the syn-eruptive lake level. (f) Renewed rise of lake level in the latter part of the oscillation causes backstepping of the topset–foreset series, with stacking of additional foreset–topset pairs resulting from continued deposition of drift and stream-supplied tephra. (g) Highest lake level is recorded by topset–foreset break of small spit illustrated in Fig. 9. The Bonneville flood takes place as the outlet gives way and is eroded during an immense outbreak flood, which lowers the lake to the Provo level (Oviatt *et al.*, 1992). *continued on p. 76*

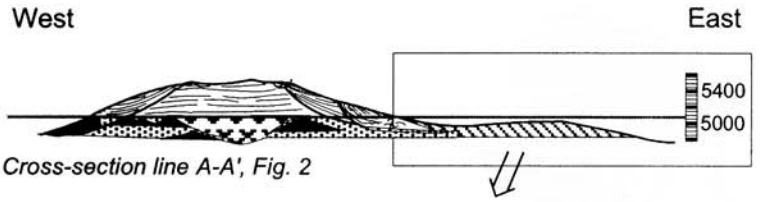

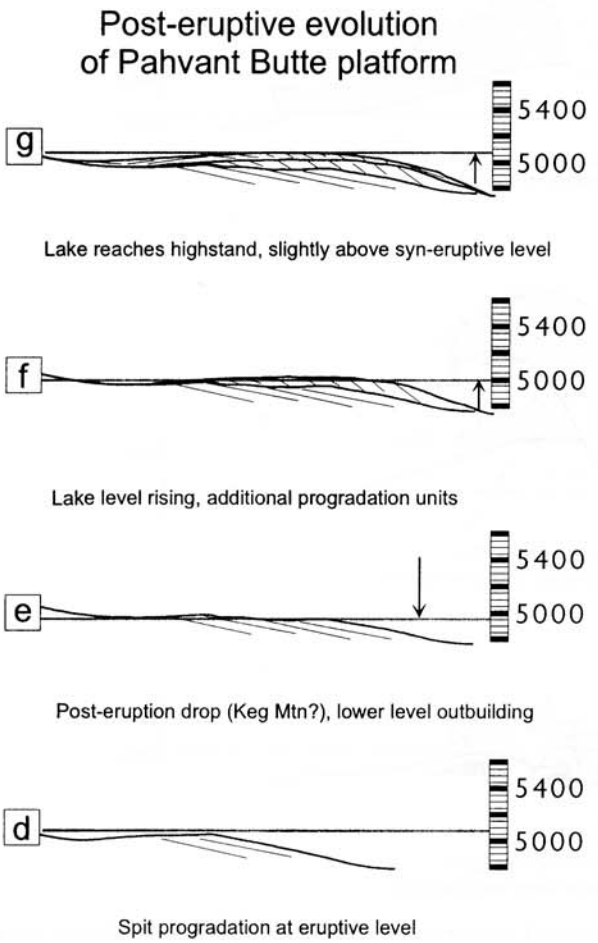

Fig. 11. (*continued*)

Eruption, emergence and construction of Pahvant Butte volcano

The Pahvant Butte eruption began beneath ≈ 85 m of water (Oviatt & Nash, 1989), and gradually built a broad mound of subaqueous tephra toward the lake surface (White, 1996). Immediately adjacent to vent sites, M2 mound facies accumulated during continuous-uprush eruptive phases (Kokelaar, 1983; White, 1996) and grade upward into steeply dipping beds of a subaqueous cone rim (lower cone facies). The cones were fed by emergent tephra jets, which penetrated the water surface and fell back, carrying ash, lapilli and bombs directly to the lake surface to feed fall-avalanche grainflows (Sohn & Chough, 1993). Vent sites were not fixed during this stage and, as active venting shifted, M2 and lower cone accumulations were onlapped by other subaqueous lithofacies. Wave erosion during this time, although limited in comparison with overnight shoreline retreat of ≈ 100 m at

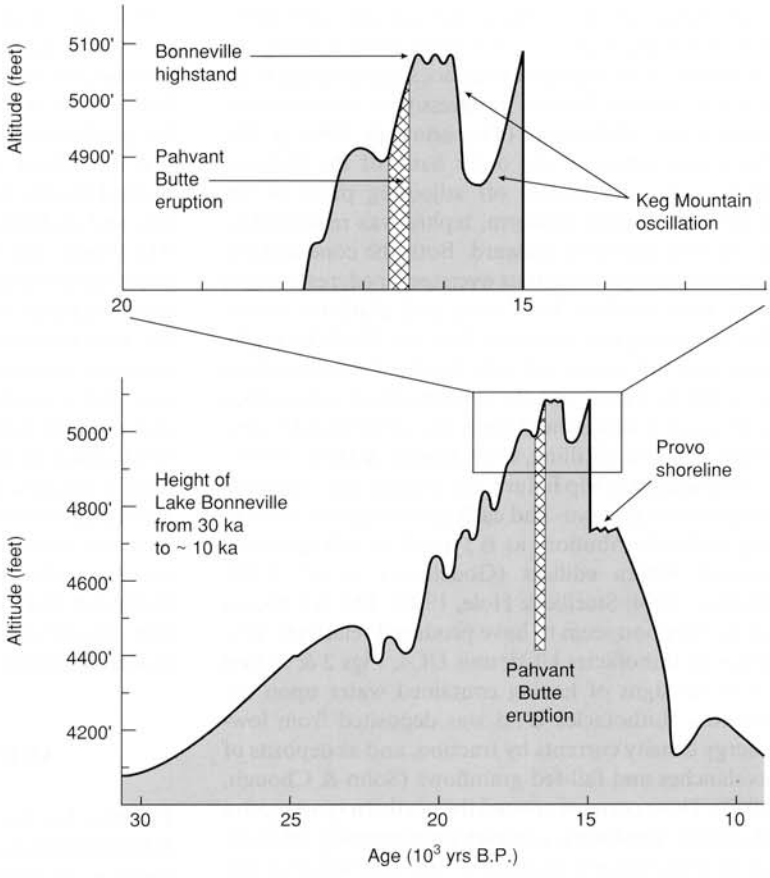

Fig. 12. Diagram showing changes in level of Lake Bonneville with time. Altitudes are in feet above sea level. (Note eruption of Pahvant Butte ash just before Lake Bonneville attained its outlet-controlled highstand level, and later variations including the significant drop and rise of the Keg Mountain oscillation (Oviatt *et al.*, 1992) before the catastrophic Bonneville Flood permanently lowered the lake by erosion of the outlet level to the so-called Provo shoreline level (prominent step *c.* 4750 ft (1448 m)).)

Surtsey (Thorarinsson, 1967), simultaneously provided material to build the platform by littoral drift.

Development of the lower cone and platform gradually increased the area of the volcano lying in shallow water, and upper cone facies began to form a subaerial tuff cone. The early deposits are predominantly of UCw facies, with abundant evidence of free water in the tephra upon deposition. This indicates that water continued to reach the vent interior in sufficient quantities to maintain a ponded Surtseyan slurry (Kokelaar, 1986) generating repeated tephra jets. Emplacement of water-laden tephra, associated with rills and failure of saturated deposits to form debris flows, is inferred to have occurred largely as direct fall from tephra jets, such as those described by Thorarinsson (1967; p. 18) to have 'ejected so much sea water over the crater rims that mud streams ran all the way down to the beach'. Thin, continuous ash beds, however, probably reflect deposition from damp, low-energy, wind-directed density currents of the sort experienced and described by Richards (1959; p. 106): 'a large black-appearing cloud poured over the graben area of the crater rim, rushed down the cone . . . particles ranged from 0.1 to 3 mm . . . dust, ash, and water mixed to form a light rain of large muddy drops, somewhat like a hailstorm . . . speed of the avalanche was about 30 knots or more.' Efficient distribution of ejecta by energetic base surges, such as occurred at Taal in 1965 (Moore *et al.*, 1966; Waters & Fisher, 1971), did not occur, with the result that a cone developed closely enclosing the vent area (Sohn, 1996).

As the Pahvant Butte eruption continued, the cone suffered slips of various magnitudes, the larger ones forming mappable discontinuities. Slip surfaces separate units UC1, UC2, and UC3 (Fig. 3), and all slips involved material entirely or predominantly of lithofacies UCw. Repeated failure along inward-dipping slips was facilitated by ejection of material from the vent area; this removed support from the base of the inner cone walls and caused material to slump into the vent, where it disaggregated and was recycled by subsequent eruptive bursts (Kokelaar, 1983). Major

slips along outward-dipping surfaces are inferred to have taken place as a result of wave erosion along the shoreline of the emergent volcano; slips resulting from wave erosion at Surtsey progressively truncated the highest part of the cone (Thorarinsson, 1967; p. 28). As waves truncated the outer flank of the Pahvant Butte cone and planed off adjoining parts of the underlying tephra platform, tephra was reworked to extend the platform outward. Both the cone and the platform margin were thus oversteepened, resulting in slips that involved both cone and platform strata. Such syn-eruptive outward slips are likely to typify emergent tuff cones; not only do they have shorelines exposed to waves, but the uncompacted subaqueous tephra upon which these cones are constructed is generally unstable (Skilling, 1994; Smellie & Hole, 1997).

In addition to slip failure, the mound and cone were subject to major syn- and early post-eruptive reworking and redistribution, as is typical of subaqueously formed tephra edifices (Godcheaux *et al.*, 1992; Skilling, 1994; Smellie & Hole, 1997). The last phases of the eruption seem to have produced relatively 'dry' deposits (lithofacies UCd; unit UC4, Figs 2 & 3) that show no signs of having contained water upon deposition. Lithofacies UCd was deposited from low-energy density currents by traction, and as deposits of avalanches and fall-fed grainflows (Sohn & Chough, 1993). These currents crossed the northern syn-eruptive shoreline, producing complex interfingering relationships with platform strata (Fig. 10). The nature of this sort of dry, low-energy density current at Surtsey was revealed by Thorarinsson (1967; p. 23): 'After each large explosion and the following bomb shower, a brown pumice-laden cloud enveloped . . . clouds were warm and cosy, the pumice grains being so light that they did not hurt . . . a peculiar circular motion whisked the pumice grains from one side to another.' A critical aspect of this account is that the ballistic showers were followed by descending 'clouds' of dry ash. The phenomenon is analogous to tephra-finger jets in the simultaneous ejection of large blocks that pass through associated ash that subsequently follows the blocks to the ground, yet condensed water droplets are absent. It is inferred that the dry ash follows the ballistic blocks as weak vertical density flows (convective settling) rather than sedimenting as by fall of individual grains, and that this produces the high particle-delivery rates needed to form fall-fed grainflows such as those represented by UCd deposits at Pahvant Butte.

Continued tephra redistribution following the eruption further built out the flat-topped platform, which surrounds and offlaps the cone and mound facies. A combination of products from surficial cone erosion and tephra that drifted around the volcano from wave-cut cliffs to the west provided the material for platform construction. Despite an extremely limited hinterland, Gilbert-type deltaic topset deposits formed locally from sediment carried off the cone in rills and shallow gullies that are no longer preserved. The topsets are related to a large foreset–clinoform sequence fed both by deltaic and beach drift processes, each shedding sediment episodically to deeper levels via sediment-gravity flows. Characteristics of these platform foresets, including relatively coarse grain size, loose packing, abundant debris-flow deposits and variable foreset dips, reflect the adjacent high-relief source of unconsolidated sand and gravel-grade tephra. Because the tephra produced by the Pahvant Butte eruption is in general highly vesicular, the grains have low densities and are easily transported relative to dense siliciclastic grains (Smith & Smith, 1985; Oehmig & Wallrabe-Adams, 1991). This resedimentation of coarse tephra could take place under even moderate-energy wave and current conditions.

ACKNOWLEDGEMENTS

Funding for this study was provided by NSF grant EAR91-05456 to R. V. Fisher, whose work on Pahvant Butte in the 1960s provided impetus and background for this study. Alec Tsongas and Stephanie Petralia assisted in the field, and Chuck Landis, Gary Smith, and Peter Kokelaar provided helpful, informative and stimulating reviews of the manuscript.

REFERENCES

Bills, B.G. & May, G.M. (1987) Lake Bonneville: constraints on lithospheric thickness and upper mantle viscosity from isostatic warping of Bonneville, Provo and Gilbert Stage shorelines. *J. geophys. Res.*, **92**, 11493–11508.

Bills, B.G., Currey, D.R. & Marshall, G.A. (1994) Viscosity estimates for the crust and upper mantle from patterns of lacustrine shoreline deformation in the Eastern Great Basin. *J. geophys. Res.*, **99**, 22059–22086.

Buck, S.G. (1985) Sand-flow cross strata in tidal sands of the Lower Greensand (Early Cretaceous), southern England. *J. sediment. Petrol.*, **55**, 895–906.

Carter, R.M., Abbott, S.T., Fulthorpe, C.S., Haywick, D.W. & Henderson, R.A. (1991) Application of global sea-level and sequence-stratigraphic models in Southern Hemisphere Neogene strata from New Zealand. In: *Sedimentation, Tectonics and Eustasy: Sea-Level Changes at*

Active Margins (Ed. MACDONALD, D.), Spec. Publs int. Assoc. Sediment., No. 12, pp. 41–65. Blackwell Scientific Publications, Oxford.

CAS, R.A.F. & LANDIS, C.A. (1987) A debris-flow deposit with multiple plug-flow channels and associated slide accretion deposits. *Sedimentology*, **34**, 901–910.

CAS, R.A.F., LANDIS, C.A. & FORDYCE, R.E. (1989) A monogenetic, Surtla-type, Surtseyan volcano from the Eocene–Oligocene Waiareka–Deborah volcanics, Otago, New Zealand: a model. *Bull. Volcanol.*, **51**, 281–298.

CHOUGH, S.K. & HWANG, I.G. (1997) The Duksung fan delta, SE Korea: growth of delta lobes on a Gilbert-type topset in response to relative sea-level rise. *J. sediment. Res.*, **67**, 725–739.

CHRISTENSEN, M.N. & GILBERT, C.M. (1964) Basaltic cones suggests constructional origin of some guyots. *Science*, **143**, 240–242.

CONDIE, K.C. & BARSKY, C.K. (1972) Origin of Quaternary basalts from the Black Rock Desert region, Utah. *Geol. Soc. Am. Bull.*, **83**, 333–352.

COOMBS, D.S., CAS, R.A.F., KAWACHI, Y., LANDIS, C.A., MCDONOUGH, W.F. & REAY, A. (1986) Cenozoic volcanism in north, east and central Otago. In: *Cenozoic Volcanism in New Zealand* (Ed. SMITH, I.E.M.), Bull. R. Soc. N.Z., **23**, 278–312. Wellington.

CROWE, B.M. & FISHER, R.V. (1973) Sedimentary structures in base-surge deposits with special reference to cross-bedding, Ubehebe Craters, Death Valley, California. *Geol. Soc. Am. Bull.*, **84**, 663–682.

CURREY, D.R. (1982) *Lake Bonneville: selected features of relevance to neotectonic analysis*. Open-file Rep. 82-1070. US geol. Surv., Denver, CO.

FARRAND, W.H. & SINGER, R.B. (1991) Spectral analysis and mapping of palagonite tuffs of Pavant Butte, Millard County, Utah. *Geophys. Res. Lett.*, **18**, 2237–2240.

FARRAND, W.H. & SINGER, R.B. (1992) Alteration of hydrovolcanic basaltic ash: observations with visible and near-infrared spectrometry. *J. geophys. Res.*, **97**, 17393–17408.

FISHER, R.V. (1977) Erosion by volcanic base-surge density currents: U-shaped channels. *Geol. Soc. Am. Bull.*, **88**, 1287–1297.

FISHER, R.V. & SCHMINCKE, H.-U. (1984) *Pyroclastic Rocks*. Springer, Berlin.

GILBERT, G.K. (1890) *Lake Bonneville*. Monogr. US geol. Surv., Reston, VA, 1.

GODCHEAUX, M.M., BONNICHSEN, B. & JENKS, J.D. (1992) Types of phreatomagmatic volcanoes in the western Snake River Plain, Idaho, USA. *J. Volcanol. geothermal Res.*, **52**, 1–25.

HAMILTON, W.H. & MYERS, W.B. (1963) Menan Buttes, cones of glassy basalt tuff in the Snake River Plain, Idaho. *US geol. Surv. Prof. Pap.*, Reston, VA, **450-E**, 114–118.

HAY, R.L. & IIJIMA, A. (1968) Nature and origin of palagonite tuffs of the Honolulu Group on Oahu, Hawaii. *Geol. Soc. Am. Mem.*, **116**, 331–376.

HEIKEN, G.H. (1971) Tuff rings: examples from the Fort Rock–Christmas Lake Valley basin, south-central Oregon. *J. geophys. Res.*, **76**, 5615–5626.

HELLAND-HANSEN, W. & MARTINSEN, O.J. (1996) Shoreline trajectories and sequences: description of variable depositional-dip scenarios. *J. sediment. Res.*, **66**, 670–688.

HOFFMEISTER, J.E., LADD, H.S. & ALLING, H.L. (1929) Falcon Island. *Am. J. Sci.*, **18**, 461–471.

HOUGHTON, B.F. & WILSON, C.J.N. (1989) A vesicularity index for pyroclastic deposits. *Bull. Volcanol.*, **51**, 451–462.

JAKOBSSON, S.P. & MOORE, J.G. (1986) Hydrothermal minerals and alteration rates at Surtsey volcano, Iceland. *Geol. Soc. Am. Bull.*, **97**, 648–659.

KANO, K. (1998) A shallow-marine alkali-basalt tuff cone in the Middle Miocene Jinzai Formation, Izumo, SW Japan. *J. Volcanol. geothermal Res.*, **87**, 173–191.

KIM, S.B., CHOUGH, S.K. & CHUN, S.S. (1995) Bouldery deposits in the lowermost part of the Cretaceous Kyokpori Formation, SW Korea: cohesionless debris flows and debris falls on a steep-gradient delta slope. *Sediment. Geol.*, **98**, 97–119.

KNELLER, B.C. & BRANNEY, M.J. (1995) Sustained high-density turbidity currents and the deposition of thick massive sands. *Sedimentology*, **42**, 607–616.

KOKELAAR, B.P. (1983) The mechanism of Surtseyan volcanism. *J. geol. Soc. London*, **140**, 939–944.

KOKELAAR, B.P. (1986) Magma–water interactions in subaqueous and emergent basaltic volcanism. *Bull. Volcanol.*, **48**, 275–289.

LEYS, C.A. (1983) Volcanic and sedimentary processes during formation of the Saefell tuff-ring, Iceland. *Trans. R. Soc. Edinburgh: Earth Sci.*, **74**, 15–22.

LORENZ, V. (1974) *Studies of the Surtsey tephra deposits*. Surtsey Research Progress Report **7**, 72–79. Surtsey Research Society, Reykjavik.

MASSARI, F. (1984) Resedimented conglomerates of a Miocene fan-delta complex, southern Alps, Italy. In: *Sedimentology of Gravels and Conglomerates* (Eds KOSTER, E.H. & STEEL, R.J.), Mem. Can. Soc. petrol. Geol., Calgary, **10**, 259–277.

MASSARI, F. & PAREA, G.C. (1988) Progradational gravel beach sequences in a moderate- to high-energy, microtidal marine environment. *Sedimentology*, **35**, 881–913.

MOORE, J.G., NAKAMURA, K. & ALCARAZ, A. (1966) The 1965 eruption of Taal Volcano. *Science*, **151**, 955–960.

MULDER, T. & SYVITSKI, J.P.M. (1995) Turbidity currents generated at river mouths during exceptional discharges to the world oceans. *J. Geol.*, **103**, 285–299.

NEMEC, W. (1990) Aspects of sediment movement on steep delta slopes. In: *Coarse-Grained Deltas* (Eds COLELLA, A. & PRIOR, D.B.), Spec. Publs int. Assoc. Sediment., No. 10, pp. 29–73. Blackwell Scientific Publications, Oxford.

NIELSEN, L.H., JOHANNESSEN, P.N. & SURLYK, F. (1988) A late Pleistocene coarse-grained spit–platform sequence in northern Jylland, Denmark. *Sedimentology*, **35**, 915–937.

OEHMIG, R. & WALLRABE-ADAMS, H.-J. (1991) Hydrodynamic properties and grain-size characteristics of volcaniclastic deposits on the mid-Atlantic ridge north of Iceland (Kolbeinsey Ridge). *J. sediment. Petrol.*, **63**, 140–151.

OLLIER, C.D. & BROWN, M.J.F. (1971) Erosion of a young volcano in New Guinea. *Z. Geomorphol.*, **15**, 12–28.

ORTON, G.J. & READING, H.G. (1993) Variability of deltaic processes in terms of sediment supply, with particular emphasis on grain size. *Sedimentology*, **40**, 475–512.

OVIATT, C.G. & NASH, W.P. (1989) Late Pleistocene basaltic ash and volcanic eruptions in the Bonneville basin, Utah. *Geol. Soc. Am. Bull.*, **101**, 292–303.

OVIATT, C.G., CURREY, D.R. & SACK, D. (1992) Radiocarbon chronology of Lake Bonneville, Eastern Great Basin, USA. *Palaeogeogr. Palaeoclimatol. Palaeoecol.*, **99**, 225–241.

OVIATT, C.G., MCCOY, W.D. & NASH, W.P. (1994) Sequence stratigraphy of lacustrine deposits: a Quaternary example from the Bonneville basin, Utah. *Geol. Soc. Am. Bull.*, **106**, 133–144.

POSTMA, G. (1984) Mass-flow conglomerates in a submarine canyon: Abrioja fan-delta, Pliocene, southeast Spain. In: *Sedimentology of Gravels and Conglomerates* (Eds KOSTER, E.H. & STEEL, R.J.), Mem. Can. Soc. petrol. Geol., Calgary, **10**, 237–258.

PRIOR, D.B. & BORNHOLD, B.D. (1989) Submarine sedimentation on a developing Holocene fan delta. *Sedimentology*, **36**, 1053–1076.

PRIOR, D.B. & BORNHOLD, B.D. (1990) The underwater development of Holocene fan deltas. In: *Coarse-Grained Deltas* (Eds COLELLA, A. & PRIOR, D.B.), Spec. Publs int. Assoc. Sediment., No. 10, pp. 75–90. Blackwell Scientific Publications, Oxford.

RICHARDS, A.F. (1959) Geology of the Islas Revillagigedo, Mexico, 1. Birth and development of Volcan Barcena, Isla San Benedicto. *Bull. Volcanol.*, **22**, 73–123.

RICHARDS, A.F. (1965) Geology of the Islas Revillagigedo, 3. Effects of erosion on Isla San Benedicto 1952–61 following the birth of Volcan Barcena. *Bull. Volcanol.*, **28**, 381–403.

SACK, D. (1989) Reconstructing the chronology of Lake Bonneville: an historical review. In: *History of Geomorphology: from Hutton to Hack* (Ed. TINKLER, K.J.), Binghamton Symposia in Geomorphology, International Series, **19**, 223–256.

SEGERSTROM, K. (1950) *Erosion studies at Paricutin volcano, State of Michoacan, Mexico.* Bull. US geol. Surv., Denver, CO, **956-A**.

SKILLING, I.P. (1994) Evolution of an englacial volcano: Brown Bluff, Antarctica. *Bull. Volcanol.*, **56**, 573–591.

SMELLIE, J.L. & HOLE, M.J. (1997) Products and processes in Pliocene–Recent, subaqueous to emergent volcanism in the Antarctic Peninsula: examples of englacial Surtseyan volcano construction. *Bull. Volcanol.*, **58**, 628–646.

SMITH, G.A. & SMITH, R.D. (1985) Specific gravity characteristics of recent volcaniclastic sediment: implications for sorting and grain size analysis. *J. Geol.*, **93**, 619–622.

SOHN, Y.K. (1996) Hydrovolcanic processes forming basaltic tuff rings and cones on Cheju Island, Korea. *Geol. Soc. Am. Bull.*, **108**, 1199–1211.

SOHN, Y.K. & CHOUGH, S.K. (1989) Depositional processes of the Suwolbong tuff ring, Cheju Island (Korea). *Sedimentology*, **36**, 837–855.

SOHN, Y.K. & CHOUGH, S.K. (1992) The Ilchulbong tuff cone, Cheju Island, South Korea: depositional processes and evolution of an emergent, Surtseyan-type tuff cone. *Sedimentology*, **39**, 523–544.

SOHN, Y.K. & CHOUGH, S.K. (1993) The Udo Tuff Cone, Cheju Island, South Korea—transformation of pyroclastic fall into debris fall and grain flow on a steep volcanic cone slope. *Sedimentology*, **40**, 769–786.

TALBOT, M.R. & ALLEN, P.A. (1996) Lakes. In: *Sedimentary Environments: Processes, Facies and Stratigraphy* (Ed. READING, H.G.), pp. 83–124. Blackwell Science, Oxford.

TAZIEFF, H. (1972) About deep-sea volcanism. *Geol. Rundsch.*, **61**, 470–480.

THORARINSSON, S. (1967) *Surtsey: the New Island in the North Atlantic.* Viking Press, New York.

VERWOERD, W.J. & CHEVALLIER, L. (1987) Contrasting types of Surtseyan tuff cones on Marion and Prince Edward Islands, southwest Indian Ocean. *Bull. Volcanol.*, **49**, 399–414.

WATERS, A.C. & FISHER, R.V. (1971) Base surges and their deposits: Capelinhos and Taal volcanoes. *J. geophys. Res.*, **76**, 5596–5614.

WERNER, R., SCHMINCKE, H.-U. & SIGVALDASON, G. (1996) A new model for the evolution of table mountains: volcanological and petrological evidence from the Herdubreid and Herdubreidarotgl volcanoes (Iceland). *Geol. Rundsch.*, **85**, 390–397.

WHITE, J.D.L. (1992) Pliocene subaqueous fans and Gilbert-type deltas in maar crater lakes, Hopi Buttes, Navajo Nation (Arizona), USA. *Sedimentology*, **39**, 931–946.

WHITE, J.D.L. (1996) Pre-emergent construction of a lacustrine basaltic volcano, Pahvant Butte, Utah (USA). *Bull. Volcanol.*, **58**, 249–262.

WOHLETZ, K. & HEIKEN, G. (1992) *Volcanology and Geothermal Energy*. University of California Press, Berkeley.

WOHLETZ, K.H. & SHERIDAN, M.F. (1983) Hydrovolcanic explosions II. Evolution of basaltic tuff rings and tuff cones. *Am. J. Sci.*, **283**, 384–413.